Highly enhanced hard x-ray emission from oriented metal nanorod arrays excited by intense femtosecond laser pulses

Sudipta Mondal, Indrani Chakraborty, Saima Ahmad, Daniel Carvalho, Prashant Singh, Amit D. Lad, V. Narayanan, Pushan Ayyub,* and G. Ravindra Kumar†

Tata Institute of Fundamental Research, 1 Homi Bhabha Road, Mumbai 400 005, India

J. Zheng and Z.M. Sheng‡

Key Laboratory for Laser Plasmas of the Ministry of Education of China and Department of Physics, Shanghai Jiao Tong University, Shanghai, People's Republic of China

(Received 18 June 2010; revised manuscript received 7 December 2010; published 14 January 2011)

We report a 43-fold enhancement in the hard x-ray emission (in the 150–300 keV range) from copper nanorod arrays (compared to a polished Cu surface) when excited by 30-fs, 800-nm laser pulses with an intensity of 10^{16} W/cm^2. The temperature of the hot electrons that emit the x rays is 11 times higher. Significantly, the x-ray yield enhancement is found to depend on both the aspect ratio as well as the cluster size of the nanorods. We show that the higher yield arises from enhanced laser absorption owing to the extremely high local electric fields around the nanorod tips. Particle-in-cell plasma simulations reproduce these observations and provide pointers to further optimization of the x-ray emission.

DOI: 10.1103/PhysRevB.83.035408 PACS number(s): 61.82.Rx, 61.80.Ba, 61.05.−a, 52.38.Ph

I. INTRODUCTION

The interaction of intense (>10^{16}W/cm^2) femtosecond laser pulses with solid density plasmas not only provides interesting opportunities for the study of high-energy density physics,[1] but also facilitates the design of novel, micrometer-sized, femtosecond x-ray, electron, and ion sources.[2] There is tremendous interest in such tabletop pulsed x-ray sources for probing ultrafast real-time dynamics in physical and chemical systems, microscale imaging, probing dense plasma, and lithography, to name a few of the multifaceted applications.[3,4] Such exciting possibilities have led to an increasingly vigorous search for brighter sources and novel excitation schemes. The hard x-ray emission is mainly caused by hot electrons that are produced by collisionless laser absorption processes in the solid plasma.[5] The absorption is usually limited to ∼50%, which implies that approximately half the input laser energy is not utilized, necessitating the use of powerful lasers that necessarily operate at low repetition rates. The quest, therefore, is to achieve maximal coupling of laser light to the solid target, such that lower-intensity, higher-repetition-rate (say, kHz) femtosecond lasers can be used to excite these x-ray sources. It has been established during the past few years that nanostructured solid surfaces enhance the absorption of even moderately intense laser light.[6–8] In fact, near complete absorption (93%) has been recently achieved,[9] paving the way for efficient hot-electron generation and brighter x-ray sources at laser intensities that can be readily achieved by multikilohertz lasers. This high level of absorption is achieved by enhancing the local electric fields in the vicinity of the nanostructures, which leads to greater ionization and plasma absorption.[7,8,10] The local electric-field enhancement is easily understood in terms of the well-known "lightning rod" effect.[11,12] The local-field enhancement is a purely electromagnetic interaction resulting from the curvature of the nanoparticle. In addition, an applied field can induce collective oscillations of the electrons in this nanostructure, whose resonance can produce large local-field enhancement.[13]

The crucial issue to be addressed now is the precise design of the dimension and morphology of the nanostructured surface that optimizes the x-ray yield in a practically useful way. The specific type of nanostructured surface that we study here is a metal nanorod array, which consists of a large collection of nearly parallel nanorods with a fixed diameter ($2r$), adjustable height (h), and hence controllable aspect ratio ($h/2r$). We demonstrate the suitability of such a metal nanorod array as a target that acts as an efficient source of hot electrons and hard x rays at a relatively modest input laser intensity of $\sim 10^{16}$W/cm^2. The properties of such nanorod arrays are governed by either (i) additive or (ii) emergent behavior.[14] In the former case, the array may just amplify a certain advantageous property shown by a single nanorod, and thus make it practically useful. More interestingly, a nanorod array may show distinctly different properties (emergent behavior) that necessarily involve the presence of the *array*, and would *not* be observed from a single nanorod. We show here that—in addition to the aspect ratio of the nanorods—the interaction and proximity between the nanorods in the array also has an important role to play in the laser-induced x-ray emission process.

The nanorod array target was fabricated by a standard self-assembly process and is therefore amenable to batch production with well-controlled dimensional parameters. The fabrication process should essentially satisfy two critical conditions: (i) The nanorods should have a suitably high aspect ratio of well over 100, and (ii) the nanorods should be aligned approximately parallel to each other, such that the laser beam "sees" their tips. Because most chemical and vapor deposition techniques yield a random mesh of nanorods, we utilized a fabrication process based on electrochemical growth within a commercially available porous anodic alumina (PAA) template. This method provides adequate control over the length and diameter of the nanorods and naturally yields a parallel array. Experiments were done with copper nanorod arrays of four different aspect ratios. The rod diameter was

∼260 nm in all cases, while their average heights were varied in the 10–60 μm range. In the best cases, we could obtain x-ray yield enhancements of up to 43 times when compared to optically polished Cu targets. Previous studies using nanostructured surfaces have yielded enhancement factors up to 13 in the hard x-ray regime.[7] We present two-dimensional (2D) particle-in-cell (PIC) plasma simulations to further understand the data and strengthen the potential of nanorod array targets as bright, hard x-ray emitters.

II. NANOROD TARGET FABRICATION

The copper nanorod arrays were electrochemically grown within commercially available PAA templates (Whatman Anodisk), with a diameter of either 13 or 50 mm and a thickness of 60 μm, containing parallel cylindrical pores. The PAA templates were back-plated with a ∼200 nm Cu layer that served as a working electrode during electrodeposition. The nanorod arrays were electrodeposited potentiostatically in an acidic copper sulphate bath (pH = 2.0) using a 99.9% pure Cu plate as the counterelectrode. The PAA template was then removed in a basic etchant (1M NaOH) and the samples rinsed in de-ionized water. The diameter of the electrodeposited nanorods is dictated by the pore size of the PAA template (∼260 nm), while the rod length was varied by controlling the deposition time. Freestanding metal nanorods, produced by completely etching out the template, exhibit a tendency to cluster owing to the capillary force of the liquid between them. The nature and extent of clustering depend on the length of the nanorods and the nature of the drying process.[15] Here, we report laser-induced x-ray emission from both clustered and unclustered nanorod arrays with different aspect ratios. Figure 1 shows scanning electron micrographs (SEMs) of two of the typical nanorod array samples studied. While Figs. 1(a) and 1(b) represent, respectively, the surface and cross-sectional SEM images of slightly clustered Cu nanorod arrays, Figs. 1(c) and 1(d) represent the corresponding images of a heavily clustered nanorod array.

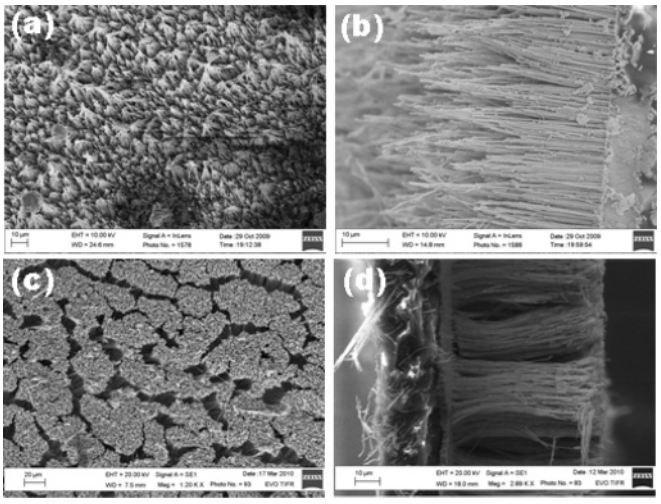

FIG. 1. Typical SEM images of Cu nanorod arrays: (a) and (b) show surface and cross-sectional views, respectively, of a nanorod array (sample 2) with an aspect ratio that equals 162; (c) and (d) show surface and cross-sectional views, respectively, of a nanorod array (sample 4) with an aspect ratio that equals 192. Note that the sample shown in (c) and (d) exhibits extensive clustering of nanorods.

III. EXPERIMENTAL SETUP

The Tata Institute of Fundamental Research (TIFR) Ti-sapphire chirped pulse amplification laser system (30 fs, 10 Hz, 800 nm) was used for plasma formation. The nanosecond prepulse contrast of the pulses was $\sim 3 \times 10^{-6}$. The pulsed laser beam was focused in $f/4$ geometry at an incident angle of 40° by an off-axis parabolic mirror to a focal spot of 17 μm on targets kept at a base pressure of 10^{-6} Torr in a vacuum chamber.

The optically polished targets (size: 50 mm × 50 mm × 5 mm) and the nanorod array targets (13 or 50 mm disks pasted on a 50 mm × 50 mm × 5 mm Cu block) were mounted side by side in a vacuum chamber and could be moved by a motorized precision stage to ensure that each laser pulse encountered a fresh portion of the target. A sample size larger than this can also be used either by direct fabrication of larger pieces or by a combination of smaller pieces. Measurements of hard x-ray emission in the 150–300 keV range were performed with a calibrated NaI (Tl) detector, followed by a photomultiplier tube. The detector was enclosed by an Al case and kept inside a thick lead cylinder. The whole arrangement was kept outside the vacuum chamber in front of a 5-mm perspex window looking at the target normally (as shown in Fig. 2). We put lead apertures in front of the detector to control the photon flux. The signal from the detector was amplified and collected by a multichannel analyzer (MCA) attached to a computer. To reduce x-ray pileup (the detector cannot distinguish between multiple photons of lower energy and a single photon of corresponding higher energy) we restrict the x-ray count level to 0.1 photon per laser shot. We triggered the MCA synchronously with the laser pulse and time gated it to eliminate noise from the cosmic ray.[16] To ensure background-free detection, we left our detection system for several hours before the experiment and noticed

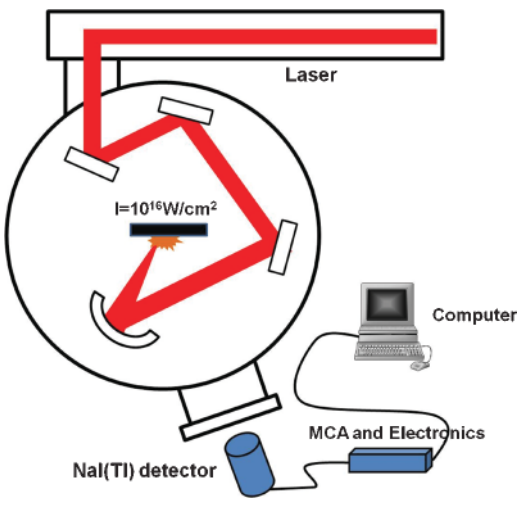

FIG. 2. (Color online) Schematic of the experimental setup.

TABLE I. Correlation between the x-ray yield enhancement and the structural parameters of five different copper nanorod array samples. The nanorod diameter ($2r$) is constant (0.26 μm) for all samples.

Sample No.	Nanorod length h (μm)	Aspect ratio $h/2r$	Cluster size (μm)	X-ray yield compared to polished Cu	Number of x-ray photons/laser shot/Sr (150–300 keV)
Polished Cu	0	0	NA	1	8.6×10^3
1	10	39	Unclustered	×14	1.2×10^5
2	42	162	6	×21	1.8×10^5
3	50	192	31	×16	1.4×10^5
4	50	192	40	×43	3.7×10^5
5	60	231	30	×36	3.1×10^5

very few counts. To control the count rate, we changed the solid angle of exposure by varying the size of the lead aperture (from 2 to 10 mm diam) placed in front of the detector. The target-detector distance was adjusted between 170 and 200 cm for different measurements. The total x-ray photons per shot per unit solid angle are shown in Table I—the total number of x-ray photons captured in the detector is calculated by summing the number of photons in each channel of MCA (over the range of 150–300 keV).

IV. RESULTS AND DISCUSSION

Figures 3 and 4 represent the bremsstrahlung emission spectra recorded from two of the Cu nanorod array targets with different aspect ratios. Similar spectra from optically polished Cu targets are displayed for comparison. In all cases, the bremsstrahlung yields from the nanorod targets are over an order of magnitude higher than those from the polished Cu targets. Table I summarizes the observed enhancement in the bremsstrahlung emission from five Cu nanorod array targets with different aspect ratios and cluster sizes. It also shows the total number of x-ray photons (per laser shot) in the 150–300 keV region assuming isotropic emission. All the Cu nanorod array samples produce ~20–40 times higher x-ray yield than the optically polished Cu targets. By comparing samples 2 and 4, we observe that the aspect ratio of sample 4 is only 18% higher, but it shows extensive clustering. Hence the much larger (more than twice) x-ray yield from sample 4 can be ascribed mainly to the clustering behavior. A similar conclusion may be drawn by comparing samples 3 and 4, which have identical aspect ratios but quite different cluster sizes. On the other hand, when we compare samples 1 and 2 (which are both virtually unclustered), we find that it is the larger (more than four times) aspect ratio of sample 2 that is responsible for its higher x-ray yield. Thus, our data definitely indicates that the x-ray enhancement depends on both the aspect ratio as well as the extent of clustering. However, it is clear that much more data are required to establish the *quantitative nature* of the correlation. What makes this a rather complicated problem (and hence outside

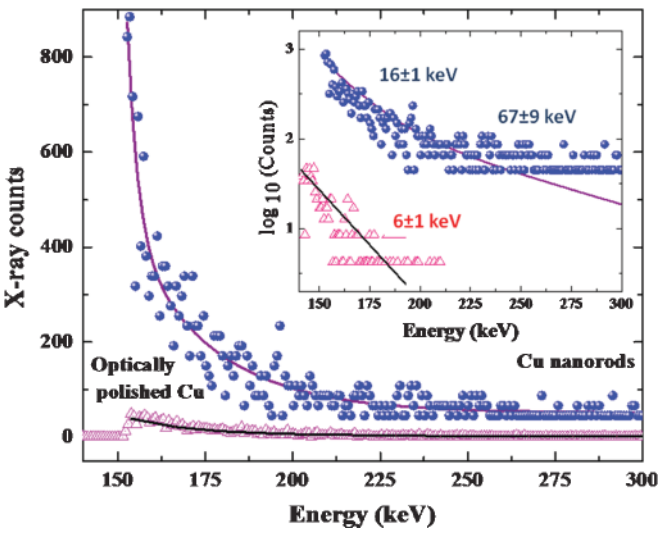

FIG. 3. (Color online) Comparison of bremsstrahlung emission from polished copper (open triangles) and copper nanorod array targets with an aspect ratio $(h/2r) = 162$ (closed circles), which resembles sample 2 (see Table I). The inset shows the logarithmic plot of the bremsstrahlung emission.

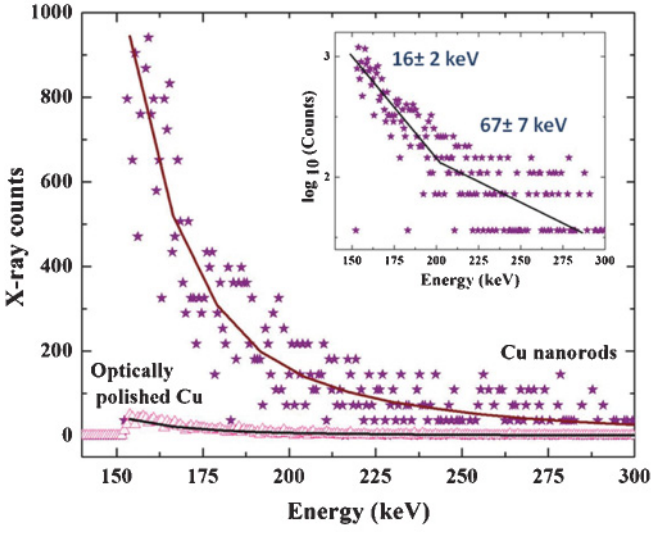

FIG. 4. (Color online) Comparison of bremsstrahlung emission from polished copper (open triangles) and copper nanorod array targets (filled stars) with an aspect ratio $(h/2r) = 231$, which resembles sample 5 (as per Table I). The inset shows the logarithmic plot of bremsstrahlung emission.

the scope of the present article) is that nanorod length is also correlated to the cluster size[15] and cannot always be independently controlled at the fabrication stage. We also point out an apparent inconsistency between the enhancement factors obtained from samples 2 and 3. This only implies that the enhancement depends not only on the aspect ratio and cluster size but probably also on other parameters such as the distance between rods within a cluster.

The insets in Figs. 3 and 4 show the values of the hot-electron temperatures obtained from the x-ray spectra. In the case of copper nanorods, two temperature components at 16 ± 2 and 67 ± 7 keV are observed. In comparison, the x-ray spectrum of the optically polished Cu target yields a temperature of 6 ± 1 keV at an identical incident laser intensity, the same as that reported in our previous studies.[7,16–18] Note that the nanorod array targets give a much higher hot-electron component of 67 ± 7 keV, while the lower component at $\sim 16 \pm 2$ keV is also substantially enhanced with respect to the unstructured targets.

As pointed out earlier, the intense laser pulse ionizes the solid target and is further absorbed by plasma absorption processes—collisional (inverse bremsstrahlung) as well as collisionless, such as resonance absorption (RA).[19] At high intensities and high densities, the collisionless absorption processes are more efficient and deplete most of the input laser energy. RA results from the damping of collective plasma waves driven by a *p*-polarized laser pulse, the absorbed energy being converted into the kinetic energy of "hot" electrons, called thus because their temperature is much larger than the energy of the majority of the electrons ($\sim$0.1 keV at 10^{15} W/cm^2). These hot electrons can then radiate out energy in the form of bremsstrahlung. The hot-electron temperature from RA is given by the well-known scaling law, $T_{\rm hot}\,({\rm keV}) = 14\left(T_c I\lambda^2\right)^{0.33}$, where T_c is the bulk plasma electron temperature in keV at the critical density, I is the intensity of the laser in units of 10^{16} W/cm^2, and λ is the wavelength of the laser in micrometers.[5,20]

V. NUMERICAL SIMULATIONS

To understand the enhanced absorption process, we take recourse to 2D PIC simulations of the plasma created on the nanorod target. The simulation box used is shown in Fig. 5. The structural parameters are taken from the experiment and slightly optimized to ensure smooth computation. The 2D PIC simulations of laser interaction were actually carried out with grating targets that resemble the nanorod-coated surface. We have taken the laser pulse with a duration of ten laser cycles and normalized amplitude $a_0 = 0.09$, corresponding to a laser intensity of 10^{16} W/cm^2 for the laser wavelength 800 nm. The initial density of the target plasma is $5n_c$. We take a grating target of 20 laser wavelengths' thickness without preplasma [see Fig. 5(a)]. The period is 0.56 laser wavelength. The width of the nanorod is 0.1 laser wavelength. The laser is incident to the target with an angle of 40°. The electron energy distribution is plotted in Fig. 5(b), which shows two components with temperatures given by 18 and 65 keV. These are close to the experimentally measured values of 16 ± 2 and 67 ± 7 keV, respectively. The higher temperature is enhanced ten times

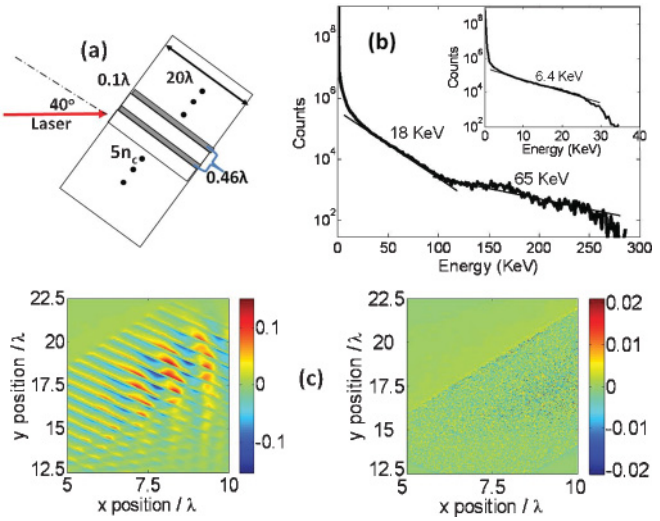

FIG. 5. (Color) (a) The sketch of the target in our 2D PIC simulation with array height $h = 20\lambda$, rod diameter $2r = 0.1\lambda$, and array period $d = 0.56\lambda$. (b) Electron energy distribution at the time when the incident laser pulse leaves the nanorod target surface. The inset shows the electron energy distribution for the plane target case. (c) The electric-field distribution after the incident laser pulse leaves the nanorod target surface (left-hand side) and the plane target surface (right-hand side).

as compared with the plane target surface case [see the inset in Fig. 5(b)]. The electric-field distributions after the incident laser pulse leaves the nanorod target surface and the plane target surface are plotted in Fig. 5(c). It is shown that the electric field generating the hot electrons in the nanorod target case is almost ten times than of the plane target case. The PIC simulations are thus able to reproduce the data very well and can be further used to optimize the shape and size of the nanorod array.

VI. CONCLUSION

We demonstrate that an array of Cu nanorods produces highly enhanced hard x-ray (150–300 keV) emission: more than 40 times larger than that from polished Cu targets under excitation by moderate intensity (10^{15}–10^{16} W/cm^2), 30-fs laser pulses. The enhancement is shown to depend jointly on the aspect ratio of the nanorods and on the nature of their clustering. It is necessary to emphasize the importance of the observed dependence of the x-ray yield on the clustering of the nanorods. This is possibly related to the presence of the so-called "hot spots" that are believed to form in the space between proximate nanostructures, and can be linked to other important phenomena such as surface-enhanced Raman scattering that also involve such hot spots. The nanorod array targets generate much hotter electrons (with a temperature of $\sim$67 keV) than the polished Cu targets (temperature $\sim$6 keV). The amplification of the local electric fields near the nanostructured surface results in increased absorption and enhanced x-ray production. The enhanced coupling of light to the laser-created solid plasmas can be understood by simple geometrical enhancement of local electric fields as well as

2D PIC plasma simulations. The significant reduction in the incident laser intensity, as well as the higher x-ray emission that are observed with nanostructured surfaces, promises multikilohertz, femtosecond, tabletop hard x-ray sources that should find applications in basic physics as well as frontline technologies.

ACKNOWLEDGMENTS

G.R.K. acknowledges a DAE-SRC-ORI grant. Z.M.S. acknowledges support from the Natural Science Foundation of China (Grants No. 10734130 and No. 10935002) and National Basic Research Program of China (Grants No. 2007CB815100 and No. 2009GB105002).

*pushan@tifr.res.in
†grk@tifr.res.in
‡zmsheng@sjtu.edu.cn

[1] R. P. Drake, *Introduction to High-Energy-Density Physics* (Springer, Berlin, 2006).
[2] G. Mourou, T. Tajima, and S. V. Bulanov, Rev. Mod. Phys. **78**, 309 (2006).
[3] W. Chao, B. H. Harteneck, J. A. Liddle, E. H. Anderson, D. T. Attwood, Nature (London) **435**, 1210 (2005).
[4] A. Bonvalet, A. Darmon, J. C. Lambry, J. L. Mattin, and P. Audebert, Opt. Lett. **31**, 2753 (2006).
[5] P. Gibbon, *Short Pulse Laser Interactions with Matter: An Introduction* (Imperial College Press, London, 2005).
[6] G. Kulcsar, D. AlMawlawi, F. W. Budnik, P. R. Herman, M. Moskovits, L. Zhao, and R. S. Marjoribanks, Phys. Rev. Lett. **84**, 5149 (2000).
[7] P. P. Rajeev, P. Taneja, P. Ayyub, A. S. Sandhu, and G. R. Kumar, Phys. Rev. Lett. **90**, 115002 (2003).
[8] H. A. Sumeruk, S. Kneip, D. R. Symes, I. V. Churina, A. V. Belolipetski, T. D. Donnelly, and T. Ditmire, Phys. Rev. Lett. **98**, 045001 (2007).
[9] S. Kahaly, S. K. Yadav, W. M. Wang, S. Sengupta, Z. M. Sheng, A. Das, P. K. Kaw, and G. R. Kumar, Phys. Rev. Lett. **101**, 145001 (2008).
[10] H. A. Sumeruk, S. Kneip, D. R. Symes, I. V. Churina, A. V. Belolopetski, G. Dyer, J. Landry, G. Bansal, A. Bernstein, T. D. Donnelly, A. Karmakar, A. Pukhov, and T. Ditmire, Phys. Plasmas **14**, 062704 (2007).
[11] R. C. Smith and S. R. P. Silva, J. Appl. Phys. **106**, 014314 (2009).
[12] P. P. Rajeev, P. Ayyub, S. Bagchi, and G. R. Kumar, Opt. Lett. **29**, 2662 (2004).
[13] G. T. Boyd, Th. Rasing, J. R. R. Leite, and Y. R. Shen, Phys. Rev. B **30**, 519 (1984).
[14] P. Ayyub, J. Cluster Sci. **20**, 429 (2009).
[15] P. Bhattacharya, S. Gohil, J. Mazher, S. Ghosh, and P. Ayyub, Nanotechnology **19**, 075709 (2008).
[16] P. P. Rajeev, S. Banerjee, A. S. Sandhu, R. C. Issac, L. C. Tribedi, and G. R. Kumar, Phys. Rev. A **65**, 052903 (2002).
[17] P. P. Rajeev and G. R. Kumar, Opt. Commun. **222**, 9 (2003).
[18] P. P. Rajeev, S. Sengupta, A. Das, P. Taneja, P. Ayyub, P. K. Kaw, and G. R. Kumar, Appl. Phys. B **80**, 1015 (2005).
[19] S. Eliezer, *The Interaction of High Power Lasers with Plasmas*, Institute of Physics Series in Plasma Physics, edited by S. Cowley, P. Stott, and H. Wilhelmsson (IOP, Bristol, 2002).
[20] D. W. Forslund, J. M. Kindel, and K. Lee, Phys. Rev. Lett. **39**, 284 (1977).